Advances in Nano Research, *Vol. 4, No. 3 (2016) 181-195*
DOI: http://dx.doi.org/10.12989/anr.2016.4.3.181

Nano-Silica effect on the physicomechanical properties of geopolymer composites

H.M. Khater*

Housing and Building National Research Centre (HBNRC), 87 El-Tahreer St., Dokki, Giza, P.O. Box 1770 Cairo, Egypt

(Received April 10, 2016, Revised July 1, 2016, Accepted July 4, 2016)

Abstract. Addition of nano-SiO_2 (NS) to geopolymer composites has been studied through measurement of compressive strengths, FTIR and XRD analysis. Alumino-silicate materials are coarse aggregate included waste concrete and demolished walls with its cementing binder, cement kiln dust (CKD) used and can possess a pronouncing activation for the geopolymer reaction resulting from the high alkali contents within. Materials prepared at water/binder ratios in a range of 0.30: 0.40 under curing of 40^{o}C and 100% Relative Humidity (R.H.), while the used activator is sodium hydroxide in the ratio of 2 wt. %. First, CKD is added in the ratio from 10 up to 50 wt., %, and the demolished walls was varied depending on the used CKD content, while using constant ratio of waste concrete (40 wt., %). Second step, depending on the optimum CKD ratio resulted from the first one (40 wt. %), so the control geopolymer mix composed of cement kiln dust, demolished walls and waste concrete in the ratio (40:20:40, wt %). Nano-silica partially replaced waste concrete by 1 up to 8%. Results indicated that, compressive strengths of geopolymer mixes incorporating nano-silica were obviously higher than those control one, especially at early ages and specially with 3%NS.

Keywords: nanostructures; sol-gel growth; amorphous materials; composite materials; inorganic compounds

1. Introduction

In this new century, the Nano-structured material technology developing at an astonishing speed and will be applied extensively with many materials. As known C-S-H gel (calcium silicate hydrate) in cement is a common building material where its main hydrate product is a natural Nano-structured material (Taylor 1993, Richardson 2000, Zhang 2000). Whilst the addition of Nano-materials in cement and concrete can lead to an extra improvements in the nanostructure of hydrated building materials (Maile 2006). Unique physical and chemical properties of Nano-materials lead to the development of more effective materials than ones which are currently available (Li *et al*. 2004).

Many researchers have applied slag; fly-ash and silica fume (SF) as a pozzolana for improving cement-based materials. It is well known that SF belongs to the category of highly pozzolanic materials because it consists essentially of non-crystalline silica with a high specific surface. However, the SF activity at early ages is somewhat low according to the literature (Mitchell and

*Corresponding author, Professor, E-mail: hkhater4@yahoo.com

Copyright © 2016 Techno-Press, Ltd.
 ISSN: 2287-237X (Print), 2287-2388 (Online)

Hinczak 1998, Papadakis 1999). As the need for the development of alternative eco-friendly building materials, alkali-activated binders has been promoted by the growth of the building industry, the increased performance requirements placed upon materials, and the higher sustainability criteria applied in construction. Alkali-activated binders offers an attractive partial or complete substitution of Portland cement in the production of mortars and concretes, offering comparable performance and cost (Duxson *et al*. 2007a) while reducing greenhouse gas emissions (Duxson *et al*. 2007b).

In the activation of aluminosilicate precursors; the most relevant characteristics related to the alkali activator are: the type of alkaline salt (usually silicate or hydroxide) (Van Jaarsveld and Van Deventer 1999, Phair and Van Deventer 2001, Fernandez-Jimenez and Palomo 2005); the method of addition of the alkaline component (as a solution or in solid-state) (Yang *et al*. 2008, Yang and Song 2009, Hajimo *et al*. 2009), and the dosage of the alkali component, usually expressed as molar ratios considering the overall composition of the raw material. Additionally, it has been reported (Van Jaarsveld and Van Deventer 1999, Duxson *et al*. 2007, Fernandez-Jimenez *et al*. 2006) that the cationic alkali supplied by the alkaline solution influences the first stage of binder formation, consequently the mechanical performance of the final products. The alkali-activators conventionally used are sodium or potassium hydroxides, and/or sodium or potassium silicates (Provis 2009). Activation with K-containing solutions leads often to an increased compressive strength development as compared with Na-containing solutions, where the size and charge density of the alkali cation play an important role in controlling the rate and extent of condensation during the polycondensation or crystallization process (McCormick and Bell 1989), however, these effects are also dependent on the chemical and physical nature of the solid precursor used (Phair and Van Deventer 2001).

Calcium hydroxide effect on the mechanical as well as microstructural characteristics of alkaline activated geopolymer alumino-silicates wastes produced from demolition works were investigated by Khater (2012), where calcium compound addition improve the mechanical and microstructural properties with hydrated lime up to 10 wt., % for water cured specimens under ambient temperature, while it slightly decreases for curing at 100%R.H at 40℃. The effect of silica fume (SF) addition on properties of geopolymer materials produced from alkaline activated metakaolin and demolished waste concrete has been studied by Khater (2013a), Results indicated that compressive strengths of geopolymer mixes incorporating SF increases up to 7% substitution and then decreases up to 10% but still higher than the control mix.

On the other hand, Cement kiln dust which is an industrial waste from cement production has relatively high alkaline content which is predominant factored preventing its recycling in cement manufacture. However, these high alkalis lie in CKD could provide the necessary environment required for geopolymer activate depending on water-soluble alkalis and sulfate compounds. Utilization of cement kiln dust (CKD) with its high alkali content in the activation of geopolymer specimens to create nonconventional cementitious binders was investigated by Khater (2013b).

Based on this background, the aim of this paper is to study effect of nano-silica addition on the physico-mechanical characteristics of the resulting geopolymer materials produced from construction and demolition wastes producing cementless materials that can be applied in many building applications. Testing of the resulting geopolymer product is studied by X-ray diffraction(XRD), FTIR, compressive strength testing and drying shrinkage are conducted on pastes of geopolymer based sample, in order to generate a better understanding of the effect of the nano silica on the behavior of Geopolymerization reaction.

Table 1 Chemical composition of starting materials (Mass, %)

Oxide, % / Material	SiO_2	Al_2O_3	Fe_2O_3	CaO	MgO	SO_3	K_2O	Na_2O	TiO_2	MnO_2	P_2O_5	Cl^-	L.O.L.	Tatal	Notes
Demolished walls	76.28	2.54	2.01	9.03	0.16	1.31	0.13	0.2	0.02	--	0.02	--	7.84	99.56	--
Waste Concrete	84.09	0.23	1.54	6.23	0.14	0.06	0.31	0.74	--	--	--	--	6.59	99.94	--
By-Pass Cement Kiln Dust (CKD)-Helwan	4.91	2.12	2.40	49.30	0.61	18.50	5.73	0.32	0.18	0.01	0.08	8.58	6.50	99.73	Free Lime, CaO=15.5
Nano Silica	99.90	0.01	0.01	0.01	0.01	0.01	0.01	0.01	--	--	--	--	0.02	99.98	--

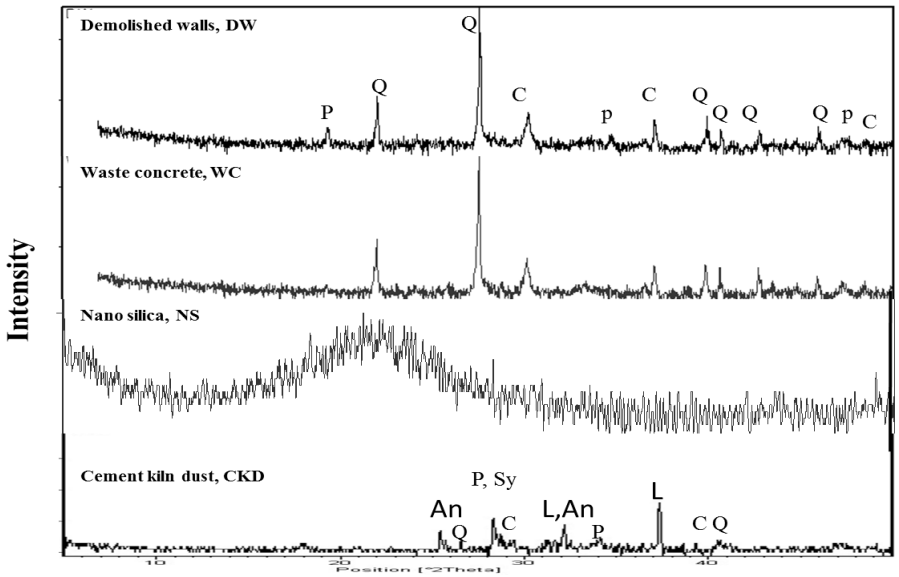

Fig. 1 XRD analysis of the used raw materials (Q: Quartz, C: Calcite, P: Portlandite, Sy: KCI, L: Lime, An: Anhydrite ($CaSO_4$))

2. Experimental procedures

2.1 Materials

Alumino silicate materials used in this investigation are demolished walls with its cementing binder as well as coarse aggregate included waste concrete both well grinded and passing a sieve of 90µm and sourced from 6th October landfills, Egypt. Cement kiln dust (CKD) which is a fine, highly alkaline powder produced from cement manufacture sourced from Helwan Cement Factory, Cairo, Egypt. Materials, which used in this investigation, were characterized by means of chemical analysis as represented in Table 1.

Mineralogical characterization was done using X-ray diffraction analysis, showing that

Table 2 Properties of nano-SiO_2

Description	Results
Diameter (nm)	8-18
Purity (%)	98
Surface area (m^2/g)	240
Density (g/cm^3)	0.5
Molecular	SiO_2
Molecular weight	60.08

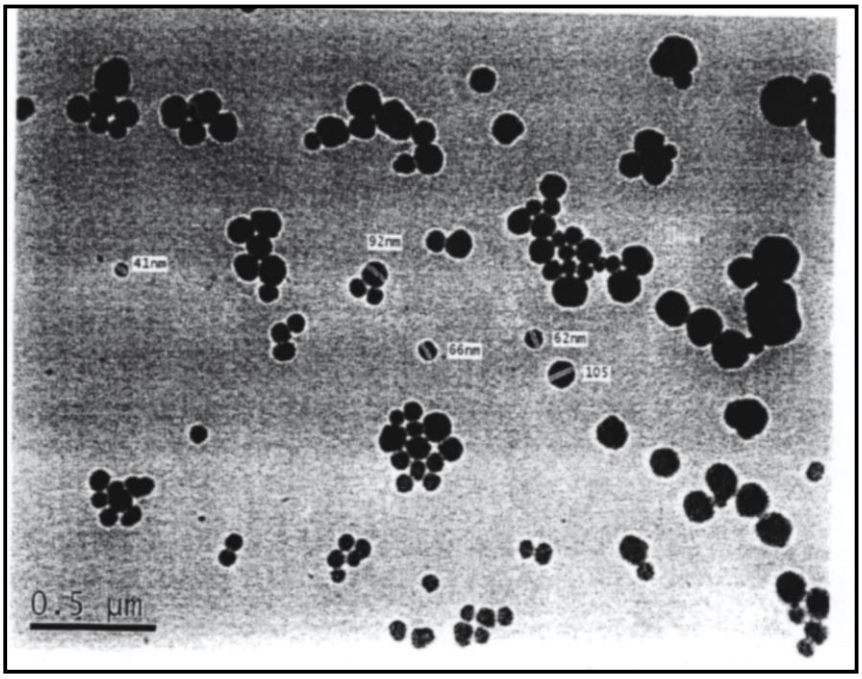

Fig. 2 Transmission electron microscopy image of nano-silica

demolished walls composed of quartz, calcite and portlandite (from cement mortar hydration) in a decreasing order. Coarse aggregate included waste concrete has a major content of quartz and little calcite content, Cement dust pattern depicts that it is composed of calcite, anhydrite, lime and a minor content from sylvite as represented in Fig. 1.

Nano-silica used in this investigation is a synthetic product with spherical particles in the range of 8-18 nm and 60 m^2/g blain fineness imported from Sigma-Aldrich (Germany). The chemical analysis showed that it consists mainly of pure silica, 99%, while its X-ray diffraction (XRD) pattern (Fig. 1) shows that nanosilica is mostly composed of amorphous quartz. The physical properties of nano-silica are given in Table 2. Laser particle size distribution pattern of nano-silica indicate that the crystallinity of NS is of an average particle size of 60 nm.

Transmission Electronic Microscopic (TEM) was carried out using type JEOL - JEM - 1230 of magnification up to 60000 to test the particle size of the used nano-silica powders. Fig. 2 shows the morphologies of NS, where its particles are represented by highly agglomerated clusters with

Table 3 Composition of the geoplymer mixes. (Mass, %)

Mix no.	Waste concrete (WC),%	Demolished walls (DW),%	Cement kiln dust, %	Nano-Silica (NS) added from the waste concrete,%	W/B ratio,%	Super-plasticizer,%	NaOH,%
C0	40.0	60	--	0	0.300	--	2
C1	40.0	50	10	0	0.320	--	2
C2	40.0	40	20	0	0.334	--	2
C3	40.0	30	30	0	0.380	--	2
C4	40.0	20	40	0	0.420	--	2
C5	40.0	10	50	0	0.434	--	2
S0	40.0	20	40	0	0.360	1.5	2
S2	39.6	20	40	1	0.360	1.7	2
S3	38.8	20	40	3	0.370	1.7	2
S4	38.0	20	40	5	0.380	2.3	2
S5	37.2	20	40	7	0.400	2.7	2
S6	36.8	20	40	8	0.420	3.0	2

size of (40-65 nm). Alkaline activator used is Sodium hydroxide (NaOH) produced by SHIDO company with 99% purity for activation and formation of geopolymer constituents.

2.2 Dispersion of Nano silica

Nano silica material was first subjected for sonication using a Fritish 450 Sonifier Analog Cell Distributor for 15 min (Collins *et al*. 2012). Gelenium Ace 30-polycarboxylate based super-plasticizer used for Nano-silica dispersion as this Polycarboxylate based superplasticizer has been proven to be effective for Nano-silica dispersion (Senff *et al*. 2013). Solutions with concentration of 0, 1, 3, 5, 7 and 8-wt., % of the used waste concrete were used to identify the effect of Nano-silica concentrations for the evaluation of its threshold ratio.

2.3 Geopolymerization and curing

Nano-particles are not easy to disperse uniformly due to their high surface energy. Accordingly, mixing was performed as follows:

1. Nano-SiO_2 particles were stirred with 50% of the mixing water using high speed magnetic stirrer for 15 min.
2. Geopolymer materials passing a sieve of 90 µm as represented in Table 3 were hand mixed with the alkaline activator solution and with the other part of mixing water for 10 minute followed by a further 5 minute using rotary mixer and mixed at medium speed (80 rpm) for another 30 s.
3. Gelenium Ace- 30 superplasticizer (Polycarboxylate based) were added and stirred with the mixture at high speed for additional 30 s, followed by the previously stirred Nano-silica.
4. The mixture allowed to rest for 90 s and then mixed for 1 min at high speed.

All investigations involved the addition of 2 wt., %NaOH of dry mixes. Water-binder material ratio (w/b) increases depending on the added nano content as indicated in the table below. The

paste mixture was casted into 25×25×25 mm cubic-shaped moulds, vibrated for compaction and sealed with a lid to minimize any loss of evaporable water.

All mixes were left to cure undisturbed under ambient temperature (23℃) for 24 hrs, demolded and then some specimens were left to be water cured under room temperature. At the end of the curing regime, the specimens were removed from their curing condition, dried well at 80℃ for 24 hrs then exposed to the compressive strength measurements, while the other parameters estimated by using the resulted crushed specimens.

2.4 Methods of investigation

Axios (PW4400) WD-XRF Sequential Spectrometer (Panalytical, Netherland) was used for Chemical analysis of the used materials. Compressive strength tests were carried out using five tones German Brüf pressing machine with a loading rate of 100 kg/min determined according to ASTM C109M (2012). Mineralogical investigation performed by using Philips PW 1050/70 XRD -Diffractometer using a Cu-Kα source with a post sample *Kα* filter. XRD patterns were collected from 0° to 50° 2Θ. Data were identified according to the XRD software (pdf-2: database on CD-Release 2005). Particle size analysis was done using a laser scattering particle size distribution analyzer (Horiba LA-950, Kyoto, Japan). Hydration stopped by subjecting crushed specimens to stopping the solution of alcohol/acetone (1:1) using stopping solution on followed by washing with acetone as recommended by different investigators (Saikia *et al*. 2004, Khater 2010) to prevent further hydration.

Transmission Electronic Microscopic (TEM) (type JEOL - JEM - 1230) used to measure the particle size of the nano. Bonding characteristics of the alkali activated specimens were analyzed using a Jasco-6100 Fourier transformed infrared spectrometer FTIR. Test sample was ground and uniformly mixed with KBr at a weight ratio KBr: specimen=200:1. The mixture, 0.20 g was pressed to a disk of 13 mm in diameter for analysis at 8 t/cm^2.The wave number was ranging from 400 to 4000 cm^{-1} (de Vargas *et al*. 2014, Panias *et al*. 2007).

3. Results and discussion

3.1 Effect of cement kiln dust on Geopolymer characterization

FTIR spectra of 28 days cured (40℃ and 100%R.H.) geopolymer specimens having various cement dust content are shown in Fig. 3. Bands description are as follow: stretching vibration of O-H bond at about 3430 cm^{-1}, bending vibration of H-O-H bond at about 1630 cm^{-1}, stretching vibration of CO_2 located at about 1430cm^{-1}, asymmetric stretching vibration (T-O-Si) at about 1100cm^{-1} where T=Si or Al, symmetric stretching vibration of CO_2 at about 870 cm^{-1}, symmetric stretching vibration (Si-O-Si) attributed to α-quartz at about 797 cm^{-1}, symmetric stretching vibration (Al -O-Si) between778-781 cm^{-1}, symmetric stretching vibration (Si-O-Si and Al-O-Si) in the region 676-688 cm^{-1} and bending vibration (Si-O-Si and O-Si-O) in the region 410-460 cm^{-}.

The pattern indicates the growth and the broadness of the main asymmetric band with CKD increase up to 40%, and then decreases with further increase. The increase in the band indicates the increased content of N-A-S-H gel which has a positive effect on strength increase. This illustrated the aluminosilicate polycondensation reactions with CKD addition up to 40%, resulting in growth of N-A-S-H gel, which contributes to an increase in mechanical properties of the

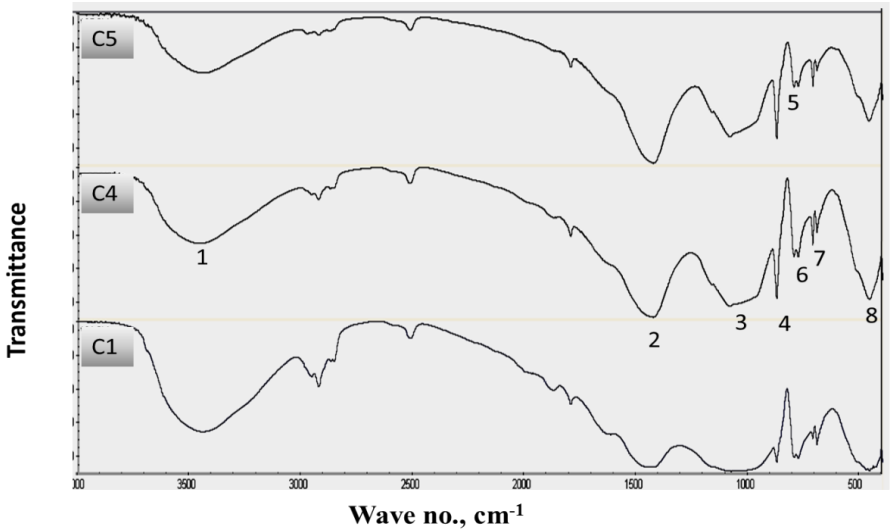

Fig. 3 FTIR spectra of 28 days cured (38℃ and 100%R.H.) geopolymer speciments having various cement dust content where: C1 has 10% CKD, C4 has 40%CKD, C5 has 50% CKD. (1: stretching vibration of O-H bond, 2: Bending vibrations of (HOH), 3: Asymmetric stretching vibration (T-O-Si), 4: Symmetric stretching vibration (Al-O-Si), 7: Symmetric stretching cibration (Si-O-Si and Al-O-Si), 8: Bending vibration (Si-O-Si and O-Si-O))

resulting structure.

Bands at about 797 cm^{-1} decreases with the cement kiln dust increase indicating the increased dissolution in α-quartz of the reacting raw materials, but the contribution of the resulting dissolved silica lowered with cement dust more than 40 % which favoring the mononuclear formation than oligomerization and polymerization where the increased alkali contents consumes the surface species (>T-OH and >T-O−), where the bonding between insoluble solid particles and the geopolymeric framework takes place. Thus, the resulted geopolymeric materials will have low mechanical characteristics (Panias *et al*. 2007, Baes and Mesmer 1976).

Bands at about 777 and 694 cm^{-1} for symmetric vibration band of (Al-O-Si) as well as the symmetric band of (Si-O-Si and Al-O-Si) are directly proportional to the asymmetric vibration band giving an indication about the increased dissolution and polymerization of aluminosilicate gel with CKD up to 40%.

The appearance of bands in the regions of 1430 cm^{-1}(ν C-O), and 867 cm^{-1}(δ C-O) are typical of $CO3^{2-}$ vibrational groups, present in inorganic carbonates (Garcia-Lodeiro *et al*. 2010), the increased intensity of carbonate with CKD is mainly due to increased carbonate in CKD and carbonation of the free alkalis lies within CKD.

Fig. 4 shows the 28 days compressive strength of geopolymer mixes cured at 40℃ and 100%R.H. It is found that, the compressive strength of geopolymer specimens increase with CKD up to 40% then decrease with further CKD increase, giving an increased mechanical strength than the control by 89.9, 112.6, 143.4 and 172% for 10, 20, 30 and 40%, respectively, while further increase in CKD up to 50% leads to increase in the alkali content in the matrix and so efflorescence occurs, however strength still higher than the control one by 67.1%

This can be explained by the high alkalis that lie within CKD lead to increase in pH of the medium and so the degree of polymerization of the resulting product. While further increase in

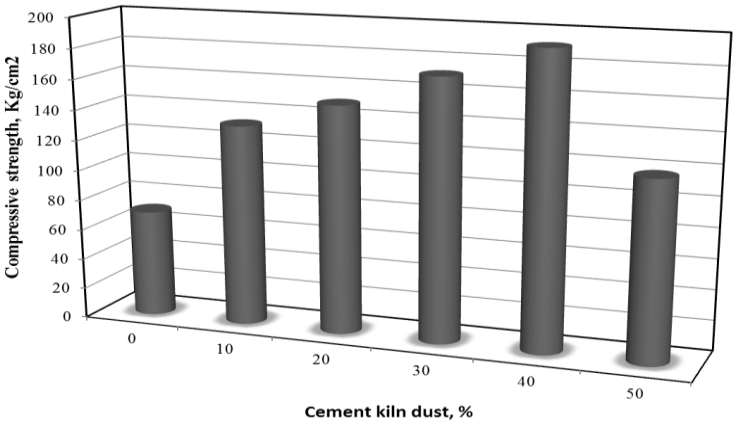

Fig. 4 Compressive strength of 28 days cured alkali activated Geopolymer specimens having various ratios of cement kiln dust

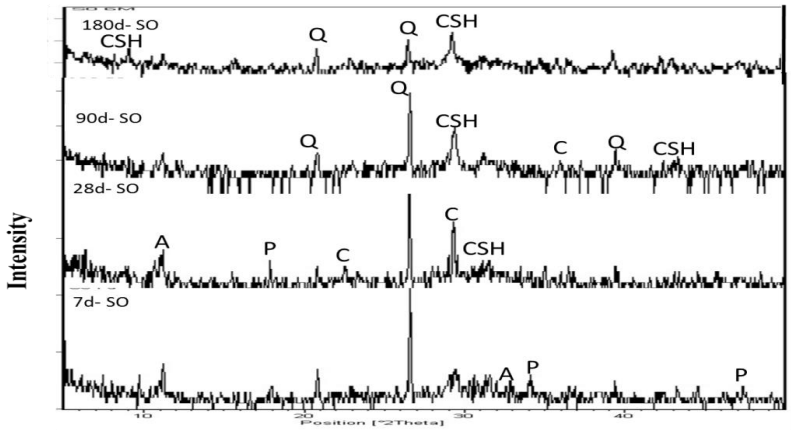

Fig. 5 XRD pattern of Geopolymer mix without Nano silica at different curing ages (Q: Quartz, A: C_4AH_{13}, C: Calcite, CSH: Calcium silicate hydrate)

CKD results in an extra alkalis increase which will negatively affect the reaction by terminating the geopolymer chains and also favor the reverse reaction for monomer formation and consuming the surface structure as mentioned before. This can illustrated well from the previously showed FTIR figure where the increased broadness and intensity of the main asymmetric peak (T-O-Si), as well as the symmetric peak of (Al-O-Si) when using 40%CKD emphasize the growth of N-A-S-H gel, which contributes to the increase in mechanical properties of the resulting structure with CKD addition up to 40%, while the reverse effect of alkali comes clear as these band lowered with increased CKD content (Baes and Mesmer 1976).

3.2 Effect of Nano-silica on Geopolymer characterization

XRD pattern of alkali-activated geopolymer mix admixed with Gelenium Ace superplasticizer and has not Nano-silica and cured at 38℃ and 100%R.H., from 1 up to 180 days is shown in Fig. 5. The pattern illustrate a broad band in the region of 6° to 10° 2θ for aluminosilicate gel and broad

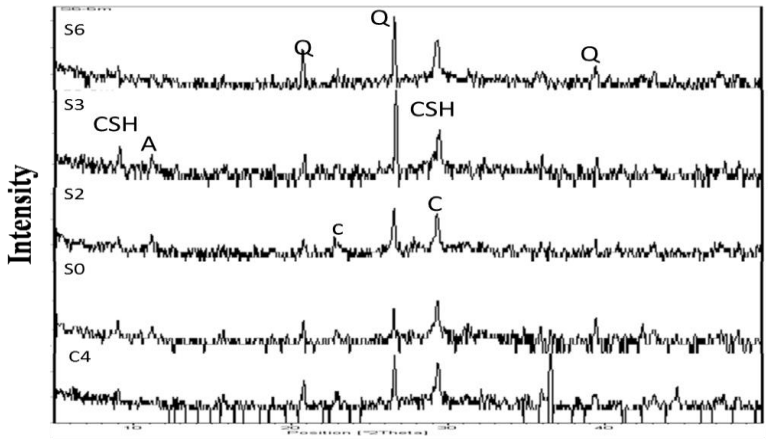

Fig. 6 XRD pattern of 180 days Geopolymer mixed having various Nano silica content (Q: Quartz, A: C4AH13, C: Calcite, CSH: Calcium silicate hydrate)

bands in the region of 17° to 35° 2θ characterizing glassy phase of geopolymer constituents. These two regions are considered as a vital role in geopolymer characterization, where any increase in these regions will be reflected on the performance and efficiency of the resulting geopolymer gel. CSH content increased with the increase of curing time as indicated from the increased broadness at 29.4° that results from the interaction of freely dissolved silica with Ca species in the matrix forming CSH, which accumulate in the open pores and transformed into crystalline form at the later curing ages, this will be in accordance with the consumption of the free portlandite content beyond 7 days. However, Aluminate phases that formed at early ages diminished with time as it dissolved into free alumina by alkaline effect and incorporated in the 3D geopolymer network, which emphasized by the increased hump in the region between 17-35° 2θ.

Addition of NS esults in the increase in the CSH phases at 29.4^o up to 3%, then decreases with further nanomaterials increase as illustrated in 180 days XRD spectra Fig. 6.where the dissolved Ca species react with the amorphous nanomaterials forming CSH that acts as a nucleating sites for formation and accumulation of dissolved species leading to a rapid hardening, forming a fine and homogeneous structure (Khater 2013a, 2013b).

FTIR spectra of the control mix that has not nano silica and admixed with Gelenium Ace Superplasticizer for 90 days are shown in Fig. 7. The spectra showed the growth of the main asymmetric band at about 950 cm^{-1} with curing time reflecting the growth of the three dimensional geopolymer network (N-A-S-H gel) with time which accompanied by the decrease in the shoulder that lies at about 1100cm^{-1} for asymmetric vibration of non-dissolved silica from the reacting materials with time; reflecting the dissolution of the reacting materials and formation of geopolymer chains (Panias *et al*. 2007)**.** There is also shoulder at about 3600 cm^{-1} for portlandite which decrease with time, forming the binding CSH phases which is in accordance with XRD pattern in Fig. 5. The spectra showed also the decrease of the carbonate content at about 1430, 870 cm^{-1} with time where the resulted geopolymer structures fill most of the open pores and mostly all the alkaline activators consumed in the geopolymer formation, where the free alkalis in the medium are susceptible to carbonation and results in formation of trona ($(Na_3H(CO_3)_2.2H_2O$) and natron ($Na_2CO_3.10H_2O$).

FTIR spectra of geopolymer mixes having various ratios of Nano-silica cured up to 90 and 180

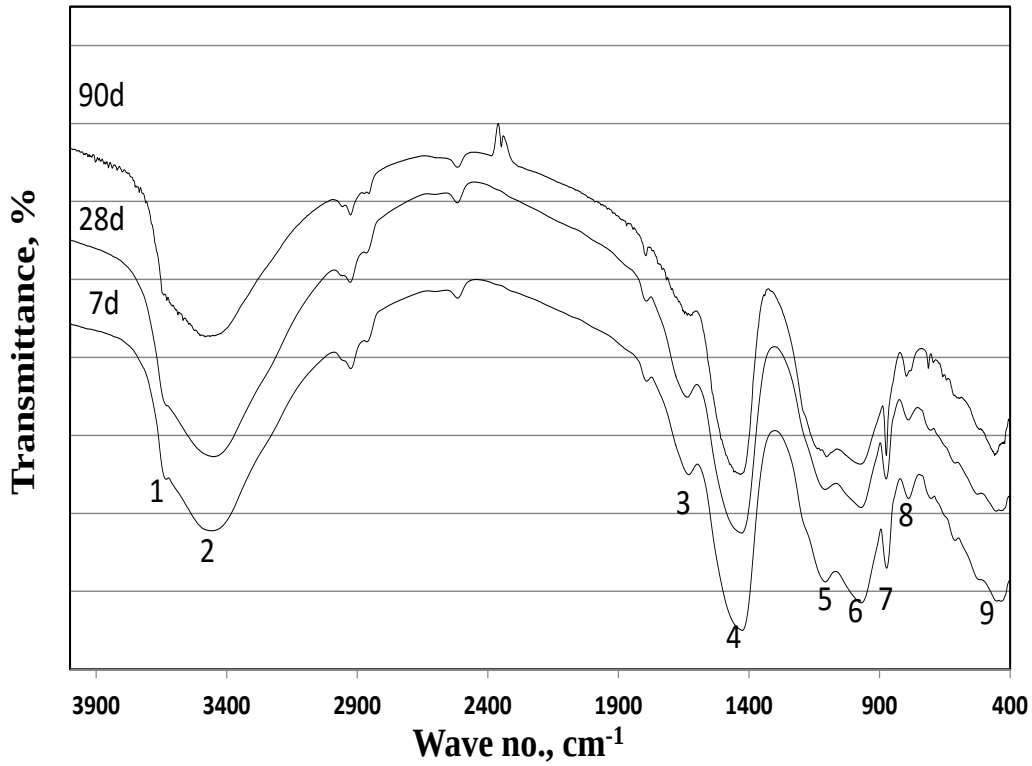

Fig. 7 FTIR spectra of control Geopolymer mix without Nano-silica, admixed with superplasticizer, cured (40℃ and 100%R.H.) at various curing times (1,2: Stretching vibration of O-H bond, 3: Bending vibrations of (HOH), 4: Stretching vibration of CO_2, 5: Asymmetric stretching vibration (Si-O-Si), 6: Asymmetric stretching vibration (T-O-Si), 7: Symmetric stretching vibration of CO2, 8: Symmetric stretching vibration (Si-O-Si) attributed to α-quartz, 9: Bending vibration (Si-O-Si and O-Si-O)

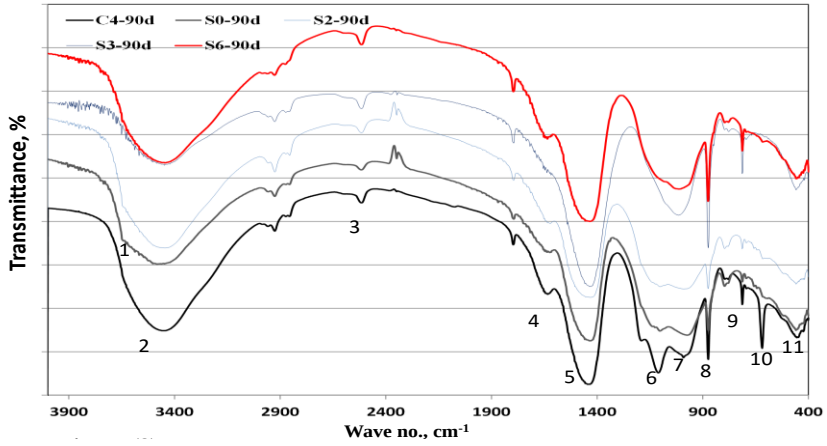

Fig. 8 FTIR spectra of 90 days cured (40℃ and 100%R.H.) geopolymer specimens having various Nano-silica content (1,2,3: Stretching vibration of O-H bond, 4: Bending vibrations of (OHO), 5: Stretching vibration of CO_2, 6: Asymmetric stretching vibration (Si-O-Si), 7: Asymmetric stretching vibration (T-O-Si), 8: Symmetric stretching vibration of CO_2, 9,10: Symmetric stretching vibration (Si-O-Si and Al-O-Si), 11: Bending vibration (Si-O-Si and O-Si-O))

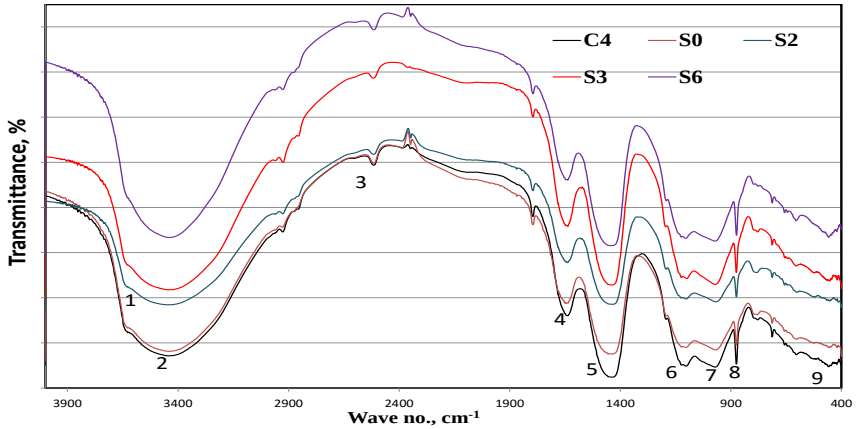

Fig. 9 FTIR spectra of 180 days cured (40℃ and 100%R.H.) geopolymer specimens having various Nano-silica content (1,2,3: Stretching vibration of O-H bond, 4: Bending vibrations of (OHO), 5: Stretching vibration of CO_2, 6: Asymmetric stretching vibration (Si-O-Si), 7: Asymmetric stretching vibration (T-O-Si), 8: Symmetric stretching vibration of CO_2, 9,10: Symmetric stretching vibration (Si-O-Si and Al-O-Si), 11: Bending vibration (Si-O-Si and O-Si-O))

days are shown in Figs. 8 and 9. Fig. 8 showed the growth of the main asymmetric band at about 950 cm^{-1} and decreased intensity of asymmetric shoulder of Si-O-Si related to non-solubilized quartz particles in raw materials with the increased dose of Nano-silica up to 3% then this asymmetric band increased again. As mentioned before, the increased intensity of asymmetric peak give an indication about the propagation and polymerization of the aluminosilicate network as the Nano-silica acts as a seeding agent for geopolymer accumulation and precipitation while further increase leads to the agglomeration of the Nano-silica leading to the formation of heterogeneous structure filled with many pores and more prone to carbonation. This confirms the decreased intensity of carbonate band with nanosilica up to 3% then increased again with further increase. The spectra illustrate also the enhanced effect of superplasticizer on the geopolymerization reaction as come clear from the asymmetric band of T-O-Si and the noticeable increase in the intensity of asymmetric Si-O-Si than admixed with superplasticizer, this will reflected positively on the mechanical characteristics of the resulting product.

Further increase in curing time up to 180 days (Fig. 9) results in an increased enhancement in the broadness of the main T-O-Si asymmetric band and decrease in the intensity of non-solubilized shoulder next to the previous band with the same sequence of the latter figure, which may be due to the increased dissolution of the reacting materials with time and incorporating in the formation of the geopolymer network (Garcia-Lodeiro *et al*. 2010)**.** The spectra showed also the decrease in the broadness and intensity of carbonate bands at about 1430, 870 cm^{-1} with Nano-silica addition as the seeding effect of nano materials leaves little pores in the matrix susceptible to carbonation and so good homogeneity in the matrix, while the agglomeration of higher dose of nanosilica (>3%) results in the increased porosity in the medium and increased carbonation depth.

Compressive strengths of geopolymer mixes that admixed with superplasticizer and that not admixed, cured up to 180 days are shown in Fig. 10. The strength pattern illustrates the presence of gap in strength values between specimens admixed with SP and those not admixed and this gap increases with time up to 180 days. This gap can be explained by the good homogeneity in the matrix structure, better rearrangement in the geopolymer network and good increased yield of the

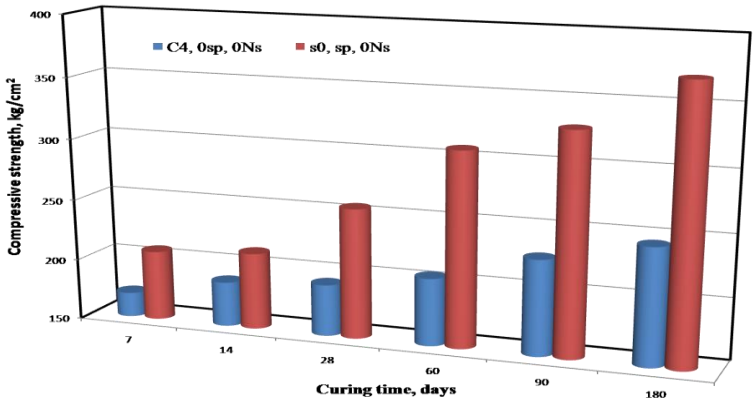

Fig. 10 Comparing the compressive strength of alkali activated Geopolymer specimens admixed and those not admixed with superplasticizer

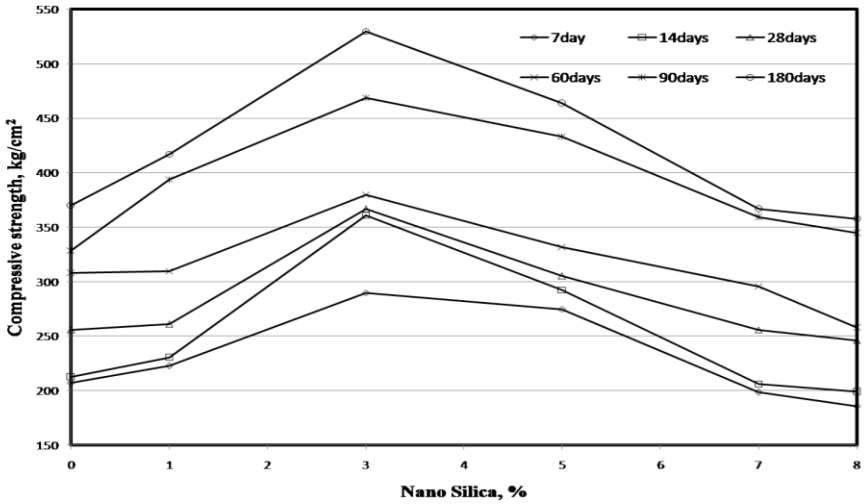

Fig. 11 Compressive strength of alkali activated Geopolymer specimens doped with various doses of Nano-silica

polymerization and precipitation. These facts confirmed by the increased content of N-A-S-H gel indicated from the asymmetric band at about 950 cm^{-1} (Figs. 8, 9) and also from the increased broadness of CSH peak in XRD pattern (Fig. 6).

Compressive strengths of geopolymer mixes that contain various ratios of Nano-silica from 0 up to 7% cured up to 180 days are shown in Fig. 11. The strength pattern illustrates the increase in strength of all mixes with curing time as a result of hydration progress forming CSH as well as geopolymer formation leading to a fine and homogeneous structure; where nano- silica has a specific surface of 160 m^2/g, so the reaction between SiO_2 and free $Ca(OH)_2$ shows differences between the geopolymer precursor carrying free lime and NS is going in quick pattern rate where NS having many unsaturated bonds Si -O and Si in the surface, the reaction process between SiO2 and $Ca(OH)_2$ may be as follows:

=Si-O- + H-OH →=Si-OH ----react quickly

=Si-+ OH →=Si-OH----react quickly

=Si-OH +Ca (OH)2→ C-S-H

Furthermore, increasing Nano-silica content up 3% leads to enhancement in seeding nucleation and possess an additional nucleation sites for the geopolymer precursors formation. It is obvious that increase in the nano-SiO_2 content beyond 3% did not change compressive strength significantly. It is found that large amounts of nano-SiO_2 decrease the compressive strength of the composites instead of improving it.

As the increased content of nano-SiO_2 leads to difficulty in dispersing uniformly ,therefore a weak zone in the form of voids is formed, consequently the homogeneous hydrated microstructure can not be formed and a lower strength will be probable (Li *et al*. 2004). Furthermore, with increasing the NS content up to 3%, geopolymer paste strength increased. For example, compared with control sample, the strengths of 3%NS increased by 39.95%, 43.3%, 42.6% and 43.1% at ages of 7 day, 28 days, 90 days and 180 days, respectively, while using 5% NS leads to strength loss by -4.2, -0.03, 9.23 and -0.94% at ages of 7 day, 28 days, 90 days and 180 days, respectively.

The trend of variation of compressive strength coincides with the XRD data, FTIR spectrum observations Figs. 8, 9, where the amorphous content of geopolymer materials increased with increasing NS content - as indicated from the increased intensity of main asymmetric T-O-Si band- as it forms more precipitation sites for geopolymer accumulation and precipitation when it interacts with free lime in the medium, forming CSH. Further increase in NS leads to insufficient wetting of the medium that hinder the propagation of geopolymer chains and so weaken its mechanical properties; as indicated from the increased carbonate content due to the increased weak zone with increased agglomeration of Nano-silica and so decrease of the intensity of amorphous band N-A-S-H as illustrated previously.

4. Conclusions

1- Cement kiln dust has high alkalis content and free lime that can efficiently be utilized in the activation of geopolymer precursors.

2- Alkaline activation of aluminosilicate wastes in addition to alkalis lies within the industrial cement kiln dust which can possess ultra-activation results in the production of environmentally friendly cementing materials that can be applied in various building purposes.

3- Uses of cement kiln dust for activation of aluminosilicate from demolition wastes can be effectively used up to 40%, while further increase leads to increase in the free alkali that can be susceptible to carbonation.

4-CKD addition to alkali activated aluminosilicate materials results in better enhancement in the Geopolymerization process up to 40%, giving increased mechanical strength than the control by 172%, while further increase leads to increase in the alkali content in the matrix and so efflorescence occurs, however strength still higher than the control one by 67.1%

5-Using nanosilica to alkali activated geopolymer specimens' increase and offers an extra nucleation sites for geopolymer formation and accumulation.

6- Adding nano silica results in the enhancement in the mechanical and functional characterization of the resulting product up to 3%, whereas further increase results in agglomeration and weakening in the mechanical characteristics.

References

Ajimohammadi, A., Provis, J.L. and Van Deventer, J.S. (2009), "One-part geopolymer mixes from geothermal silica and sodium aluminate", *Ind. Eng. Chem. Res.*, **47**(23), 9396-405.

ASTM C109M-12 (2012), Standard Test Method for Compressive Strength of Hydraulic Cement Mortars.

Baes, C.F. and Mesmer, R.E. (1976), *The Hydrolysis of Cations*, John Willey & Sons, New York.

Collins, F., Lambert, F. and Duan, W.H. (2012), "The influence of admixtures on the dispersion, workability, and strength of carbon nanotube OPC paste mixtures", *Cement Concrete Compos.*, **34**(9), 1067 74

de Vargas, A.S., Dal Molin, D.C., Masuero, Â .B., Vilela, A.C., Castro-Gomes, J. and de Gutierrez, R.M. (2014), "Strength development of alkali-activated fly ash produced with combined NAOH and $CA(OH)_2$ activators", *Cement Concrete Compos.*, **53**, 341-349.

Duxson, P., Fernandez-Jimenez, A., Provis, J.L., Lukey, G.C., Palomo, A. and van Deventer, J.S.J. (2007a), "Geopolymer technology: the current state of the art", *J. Mater. Sci.*, **42**(9), 2917-33.

Duxson, P., Mallicoat, S.W., Lukey, G.C., Kriven, W.M. and Van Deventer, J.S.J. (2007b), "The effect of alkali and Si/Al ratio on the development of mechanical properties of metakaolin-based geopolymers", *Colloid. Surf, A.*, **292**(1), 8-20.

Duxson, P., Provis, J.L., Lukey, G.C. and van Deventer, J.S.J. (2007), "The role of inorganic polymer technology in the development of green concrete", *Cement Concrete Compos.*, **37**(12), 1590-97.

Fernandez-Jimenez, A. and Palomo, A. (2005), "Composition and microstructure of alkali activated fly ash binder: effect of the activator", *Cement Concrete Compos.*, **35**, 1984-92.

Fernandez-Jimenez, A., Palomo, A. and Criado, M. (2006), "Alkali activated fly ash binders. A comparative study between sodium and potassium activators", *Mater Constr.*, **56**(281), 51-6.

Garcia-Lodeiro, I., Fernandez-Jimenez, A., Palomo, A. and Macphee, D.E. (2010), "Effect on fresh CS-H gels of the simultaneous addition of alkali and aluminum", *Cement Concrete Compos.*, **40**, 27-32.

Khater, H.M. (2010), "Influence of metakaolin on resistivity of cement mortar to magnesium chloride solution", *Ceramics-Silikáty J.*, **54**(4), 325-333.

Khater, H.M. (2012), "Calcium effect on geopolymerization of alumino silicate wastes", *J. Mater. Civil Eng.*, **24**(1), 92-101.

Khater, H.M. (2013a), "Effect of cement kiln dust on geopolymer composition and its resistance to sulphate attack", *Green Mater. J.*, **1**(Gmat1), 36-46.

Khater, H.M. (2013b), "Effect of silica fume on the characterization of the geopolymer materials", *Int. J. Adv. Struct. Eng.*, **5**(12), 1-10.

Li, H., Xiao, H.G. and Ou, J.P. (2004), "A study on mechanical and pressure-sensitive properties of cement mortar with Nano phase materials", *Cement Concrete Compos.*, **34**, 435-438.

Li, H., Xiao, H.G., Yuan, J. and Ou, J. (2004), "Microstructure of cement mortar with nano particles", *Compos. Part B*, **35**, 185-189.

Maile, A. (2006), "The chemistry and physics of nano-cement", Loyola Mary mount University, Advisor: Dr. C.P. Huang Submitted to: NSF-REU University of Delaware.

McCormick, A.V. and Bell, A.T. (1989), "The solution chemistry of zeolite precursors", *Catal Rev. Sci. Eng.*, **31**, 97-127.

Mitchell, D.R.G., Hinczak, I. and Day, R.A. (1998), "Interaction of silica fume with calcium hydroxide solutions and hydrated cement pastes", *Cement Concrete Compos.*, **28**, 1571-84.

Panias, D., Giannopoulou, I.P. and Perraki, T. (2007), "Effect of synthesis parameters on the mechanical properties of fly ash-based geopolymers", *Coll. Surf. A: Phys. Eng. Aspect.*, **301**, 246-254.

Papadakis, V.G. (1999), "Experimental investigation and theoretical modeling of silica fume activity in concrete", *Cement Concrete Compos.*, **29**, 79-86.

Phair, J.W. and van Deventer, J.S.J. (2001), "Effect of silicate activator pH on the leaching and material characteristics of waste-based inorganic polymers", *Miner Eng.*, **14**(3), 289-304.

Provis, J.L. (2009), "Activating solution chemistry for geopolymers", Eds. Provis, J.L. and van Deventer,

J.S.J., *Geopolymers: Structures, Processing, Properties and Industrial Applications*, Wood head Publishing, Abingdon UK.

Richardson, I.G. (2000), "The nature of the hydration products in hardened cement paste", *Cement Concrete Compos.*, **22**, 97-113.

Saikia, N., Usami, A., Kato, S. and Kojima, T. (2004), "Hydration behavior of ecocement in presence of metakaolin", *Res. Prog. J.*, **51**(1), 35-41.

Senff, L., Hotza, D., Repette, W.L., Ferreira, V.M. and Labrincha, J.A. (2010), "Effect of nanosilica and microsilica onmicrostructure and hardened properties of cement pastes and mortars", *Adv. Appl. Ceramic.*, **109**(2), 104-110

Taylor, H.F.W. (1993), "Nanostructure of C-S-H: current status", *Adv. Cement Bas. Mater.*, **1**, 38-46.

Van Jaarsveld, J.G.S. and van Deventer, J.S.J. (1999), "Effect of the alkali metal activator on the properties of fly ash-based geopolymers", *Ind. Eng. Chem. Res.*, **38**(10), 3932-41.

Yang, K.H. and Song, J.K. (2009), "Workability loss and compressive strength development of cementless mortars activated by combination of sodium silicate and sodium hydroxide", *J. Mater. Civ. Eng.*, **21**, 119-27.

Yang, K.H., Song, J.K., Ashour, A.F. and Lee, E.T. (2008), "Properties of cementless mortars activated by sodium silicate", *Constr. Build. Mater.*, **22**(9), 1981-9.

Zhang, X.Z. (2000), "Nanostructure of calcium silicate hydrate gels in cement paste", *J. Am. Ceram Soc.*, **83**(10), 2600-4.

JL